Suez Canal Engineering Energy and Environmental Science Journal
Faculty of Engineering – Suez Canal University
Year 2024, Volume 2, NO. 1, pages 108-127

Modeling and Performance Analysis of CERT Microgrid

Ibrahim A. Awaad[2], Naema M. Mansour[1*], Abdelazeem A. Abdelsalam[1]
[1] Electrical Engineering Dept., Faculty of Engineering, Suez Canal University 41522, Ismailia, Egypt
[2] Department of Electrical, Faculty of Engineering, Sinai University- Arish Branch, Arish, Egypt.
*Corresponding Author: E-mail: naima.mansour@eng.suez.edu.eg,
DOI: 10.21608/sceee.2024.294186.1029

Article Info:

Article History:
Received: 31\05\2024
Accepted: 22\07\2024
Published: 30\07\2024

DOI:
10.21608/sceee.2024.294186.1029

Abstract

Development in distributed energy resources (DER) technologies has opened new opportunities for on-site power generation by electricity users to cover the growing customer requirements for electric power. The Consortium for Electric Reliability Technology Solutions (CERTS) microgrid represents an entirely new approach to integrating DER. MG integration provides enhancement of reliability, power quality, and the lowering the operational costs. This paper introduces the modeling and analysis of multiple photovoltaic cells (PVs), battery storage, and controllable load within a CERTS microgrid. The operational characteristics of the simulated CERTS microgrid are investigated under different operating conditions, and a fault analysis study is carried out. The modeling stability under different operating conditions has been evaluated. The paper also offers a thorough analysis of the MG structure and the related protection and control issues The modeling and different case studies are carried out using the Matlab Simulink platform.

Keywords: *Microgrids, CERTS, photovoltaic cells, battery energy storage system, protection perspectives, energy management.*

Suez Canal Engineering, Energy and Environmental Science Journal (2024), ***2***(1), 108-127.

I.Introduction

The electrical power system gains a new dimension with the introduction of the growing use of microgrids in electricity networks, and new challenges with the operation, control, and protection of electrical networks are created. A microgrid is a group of interconnected DERs and loads that act as a single controllable entity concerning the grid. It can connect and disconnect from the grid to operate in grid-connected or island mode. However, microgrid connections can improve customer reliability and resilience to grid [1]-[9]. Challenges that arise with microgrid communications include bi-directional power flow that strongly affects the coordination of the protection system, low fault current levels during islanding mode that require an improved intelligent protection system, and frequency control during islanding operation [10], [12]. CERTS is evaluating how these resources when deployed in large numbers, affect and could be modified to enhance electricity grid reliability.

The CERT microgrid concept assumes interconnecting a group of loads and DERs that must be power electronic based to provide the required flexibility to ensure operation as an isolated system. This control flexibility allows the CERTS microgrid to present itself to the bulk power system as a single controlled unit that meets local needs for reliability and security [13]. In contrast to traditional approaches for integrating DER,

How to Cite this Article:
Awaad, I., Mansour, N. and Abdelsalam, A. (2024) 'Modeling and Performance Analysis of CERT Microgrid', Energy and Environmental Science Journal, 2(1), pp. 108–127. doi:10.21608/sceee.2024.294186.1029.

the CERTS microgrid introduced a well-controllable design to seamlessly isolate from the grid if the problems arise and reconnect once they are resolved. To fulfill these requirements, highly sensitive sensing units and high-speed switches are used to isolate the microgrid from the power system during abnormal grid conditions. This strategy allows the DER units to meet critical load demand and an advanced protection system and controller to ensure power quality and reliability [14], [15]. The CERT microgrid concept is based on some basic requirements that are summarized as:

1. Providing automatic and seamless transitions between grid-connected and islanded modes of operation to ensure load service continuity.
2. Implement an advanced protection system compatible with low fault current.
3. Implementation of an advancing control system capable of maintaining voltage and frequency stability during islanding conditions without needing an advanced communication system.

A unique feature of the CERT microgrid concept is that sensitive communication systems are not needed to control the individual DER units. Their controls automatically adapt to the new operating conditions resulting from the switch operating.

In this paper, validation of the CERTS microgrid concept is introduced by introducing a comprehensive investigation into the design, optimization, and performance analysis of an integrated microgrid comprising multiple photovoltaic (PV) cells, battery energy storage system, and AC loads with embedded controllers.

The microgrid stability is tested during different operating conditions such as grid-connected, islanding, and fault and loading conditions. Also, the control system of the microgrid is tested and evaluated during different operating conditions using the Matlab Simulink platform. A fault analysis study is carried out to reveal the operational challenges associated with microgrid connection from the protection perspective.

In section II, the cert microgrid architecture and modeling are highlighted, simulation results are discussed in section III, and the conclusion is introduced in section IV.

II.CERTS Microgrid System Architecture

According to the CERT microgrid concept, the microgrid structure assumes an aggregation of small sources and loads operating as an independent system providing electrical power. To achieve the required flexibility to ensure controlled operation as a single aggregated system, most of these sources are restricted to be power electronic-based to meet the local customers' needs related to reliability and security. Another important function of the control system is enabling the microgrid to operate in the grid-connected and islanding mode as well as a smooth transition between them [16]- [20]. An illustration of the CERT microgrid architecture is indicated in Fig. 1. The microgrid system is assumed to be a radial system with three feeders and a collection of loads. It consists of four loads (L1, L2, L3, and L4), and three distributed energy resources (two photovoltaic sources and one battery energy storage device. DER-PV1, DER-PV2, and DER-Bt.s).

The loads utilized are fixed loads , which are either capacitive or inductive. The CERTS microgrid system is connected to the grid utilizing a step-down transformer; this transformer is rated at 13.8 kV on the primary side and 0.480 kV on the secondary side [21], [22].

The four buses of the microgrid are connected via 5- feeders [T11, T22, T33, T34, T44], each feeder is 68.58. The parameters of the microgrid are indicated in Table 1. To create a well-controllable design CERTS microgrid that could seamlessly isolate from the grid, the three distributed energy resources are interfaced to the grid through a voltage source converter (VSC) which is best suited to interconnecting a microgrid to the main power grid.

Table 1 CERTS microgrid system parameters.

Transformer parameter	**Value**
T1	15.0 MVA, 60Hz, 13.8/0.48KV, X/R=6, Z=5%
L3, L4	90KW,45KVAR
L5	90KW,-40KVAR
L6	90KW,-20KVAR
Load parameter	Value
Line11, Line22, Line33, and Line 44	Size(AWG2),68.58m, 60Hz
Line34	Size(AWG2/0),22.86m
DER-PV1, DER-PV2	100KW, Unity Power Factor (3-Phase Capacitor Bank (15kVA)).

How to Cite this Article:
Awaad, I., Mansour, N. and Abdelsalam, A. (2024) 'Modeling and Performance Analysis of CERT Microgrid', Energy and Environmental Science Journal, 2(1), pp. 108–127. doi:10.21608/sceee.2024.294186.1029.

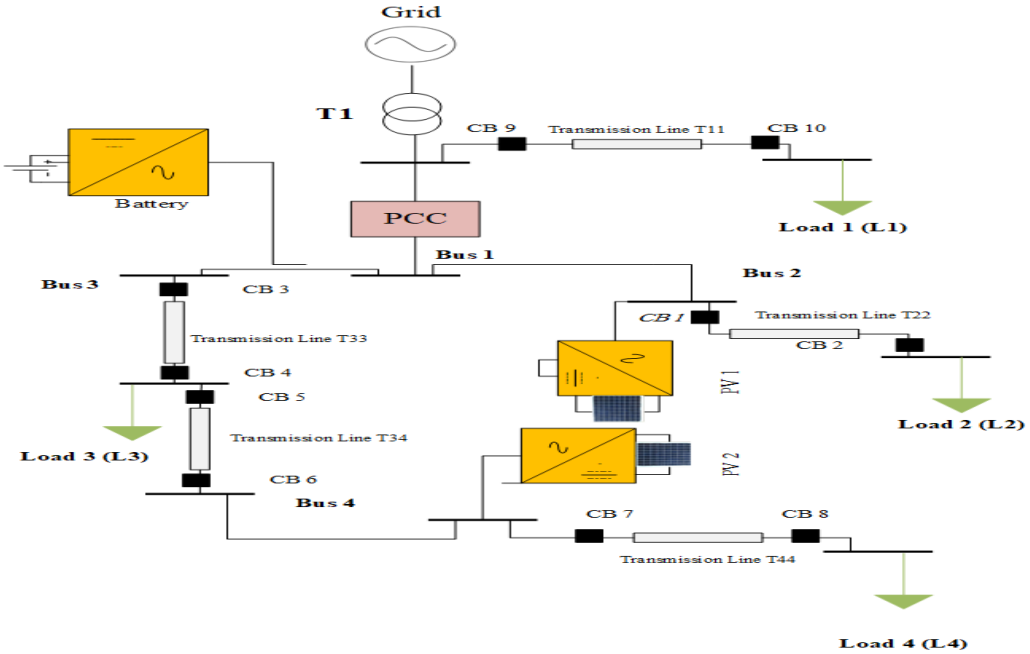

Figure. 1 CERTS microgrid Architecture.

By its capability to fast reactive power flow and voltage control at its terminals, VSC could enable a black start to energize connected microgrid or re-energizing grid; contributing to power system and voltage stability. Three different control methodologies were used to ensure the seamless transitions between grid-connected and islanded modes of the microgrid. A current-mode control with an active/reactive power controller in the dq-frame is used for battery energy storage [23]. To ensure that the maximum power is derived from the photovoltaic array, a control methodology referred to as modified-current mode control with DC link voltage is used for PV1 in grid-connected mode only and for PV2 in both grid-connected and isolated mode. For PV1 in islanding mode, frequency-mode control is used to control both the frequency and voltage. For VSC, three different control methodologies were used:

A. VSC- Current-Mode Control

Three-phase active and reactive power of the microgrid sources need to be controlled and adapted during the grid-connected mode, so the VSC-current mode controller is used. By park transformation, the three-phase quantities are transformed into a rotating d-q frame to decrease the number of control loops from three to two and facilitate the controller design and simulation. To control the power and reactive power, the line current's phase shift and amplitude are controlled. The following equations describe the basis of the transformation and controller [24].

$$\begin{bmatrix} \sin(\theta) & \sin\left(\theta-\frac{2\pi}{3}\right) & \sin\left(\theta+\frac{2\pi}{3}\right) \\ \cos(\theta) & \cos\left(\theta-\frac{2\pi}{3}\right) & \cos\left(\theta+\frac{2\pi}{3}\right) \\ \frac{1}{2} & \frac{1}{2} & \frac{1}{2} \end{bmatrix} \begin{bmatrix} V_{sa} \\ V_{sb} \\ V_{sc} \end{bmatrix} \quad (1)$$

$$P_s(t) = \frac{3}{2}\left(v_{sd}(t)i_{sd}(t) + v_{sq}(t)i_{sq}(t)\right) \quad (2)$$

$$Q_s(t) = \frac{3}{2}\left(-v_{sd}(t)i_{sq}(t) + v_{sq}(t)i_{sd}(t)\right) \quad (3)$$

Fig. 2 shows a schematic diagram of a current-controlled VSC system. In this controller mode, to adjust the active and reactive power, the three-phase VSC output currents and grid voltages are transferred from abc-to-dq0 frame to produce the control signalsv_{sd}(t), v_{sq}(t), i_d(t) and i_q(t) respectively. These signals are processed using a compensator to generate the control signals of the VSC, i.e. the modulation signals [24].

To achieve the synchronization between the VSC currents and grid voltage grid voltage's phase angle should be determined. In this model, the synchronization is performed using the phase-locked loop (PLL) method which follow quickly the variations in the grid phasing. The PLL component generates the synchronization angle that enables e the v_{sq}(t) to be kept constant at zero in the steady-state condition, facilitate the system's control, simplify the compensator design, and decrease the steady-state errors [25]. To match the system-produced real and reactive power with their required values and also to produce the reference values of current in dq-frame (i_{dref}),(if) depending on the following equations:

How to Cite this Article:
Awaad, I., Mansour, N. and Abdelsalam, A. (2024) 'Modeling and Performance Analysis of CERT Microgrid', Energy and Environmental Science Journal, 2(1), pp. 108–127. doi:10.21608/sceee.2024.294186.1029.

$$i_{dref}(t) = \frac{2}{3v_{sd}}\left(P_{sref}(t)\right) \quad (4)$$

$$i_{qref}(t) = \frac{2}{3v_{sd}}\left(Q_{\text{sref}}(t)\right) \quad (5)$$

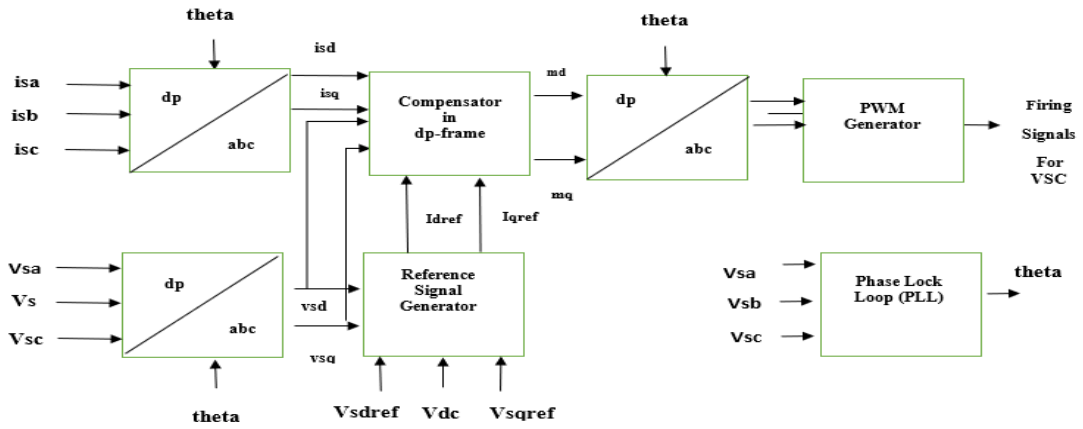

Figure. 2 Schematic diagram of a current-controlled VSC.

After that, the reference currents are generated, and fed into the compensator along with the AC side currents and AC side voltages. Converted back the output of the compensator to three phases from the dq0 frame, then fed them into the PWM generator to generate the gating signals needed for the firing of the VSC [26].

B. Controlled-Frequency VSC System

In a controlled-frequency VSC system, the voltage and frequency at the point of common coupling (PCC) are controlled during islanding mode; thus, the real and reactive power that the VSC system exchanges with the AC system are controlled.

During grid disturbance conditions, the microgrid should be isolated and operate in stand-alone mode then, is required to maintain typical frequency values on all buses and the voltage values as well. Frequency mode control methodology is used for PV1 in islanding mode as it is modeled to operate in both islanded mode and grid-connected mode. Implementation of the frequency control model for the photovoltaic source-1 PV1 is illustrated in Fig. 3 [25]- [27].

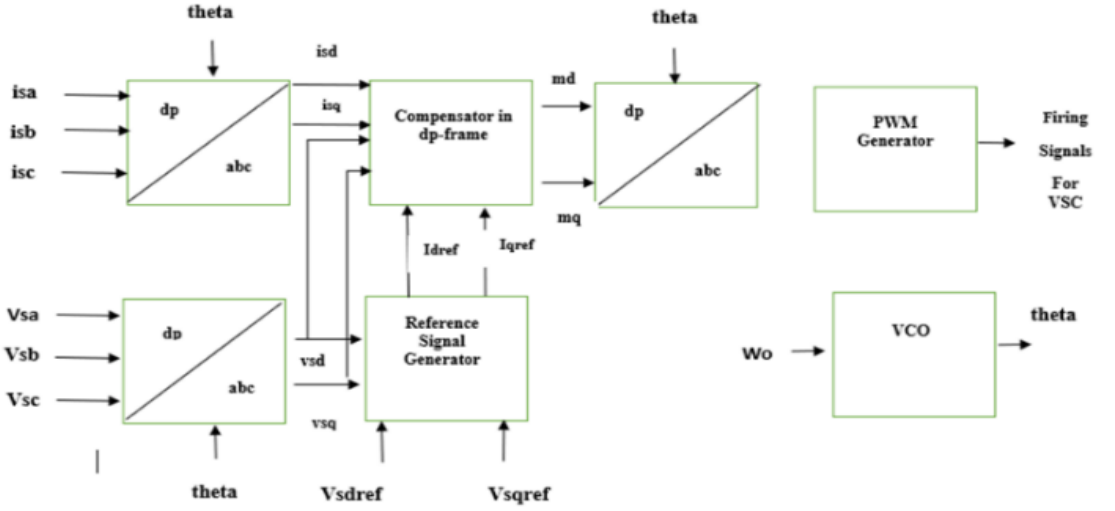

Figure. 3 Modelling of the frequency controller for the PV1.

How to Cite this Article:
Awaad, I., Mansour, N. and Abdelsalam, A. (2024) 'Modeling and Performance Analysis of CERT Microgrid', Energy and Environmental Science Journal, 2(1), pp. 108–127. doi:10.21608/sceee.2024.294186.1029.

C. Modified Current-Mode Control with DC Link Voltage

In [26- 27], the VSC current-mode control principles are discussed in detail. The enhancement in this controller is concerned with regulating of power factor of the PV system. Controlling the power generated by the PV system is achieved by controlling the DC link voltage. The objective function of the DC link voltage-control scheme is to ensure that the PV behaves in a stable manner and safe operation of the VSC. The modified current mode with DC link voltage control implementation is indicated in Fig. 4.

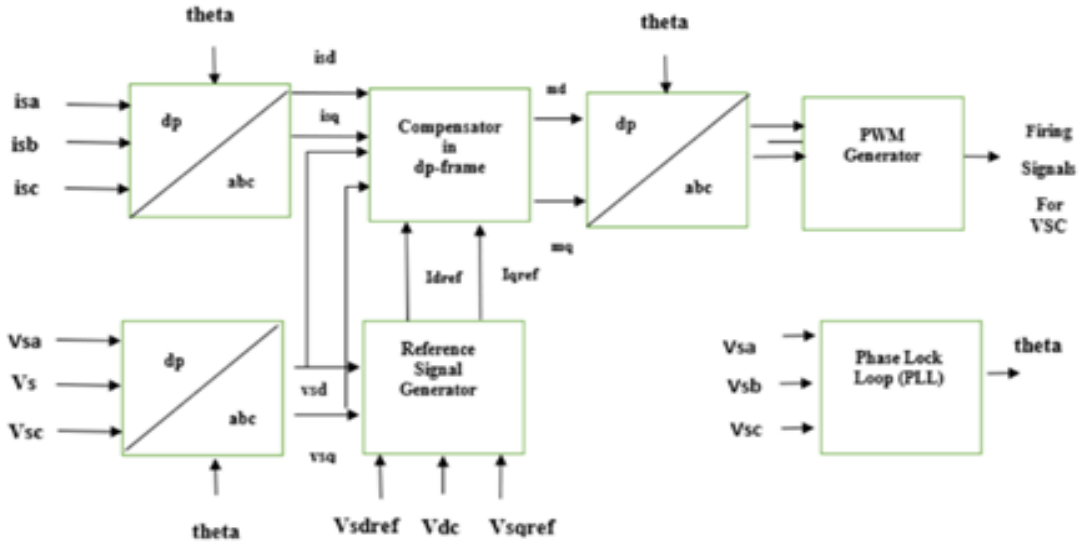

Figure. 4 Modified current-mode control with DC link voltage schematic diagram.

III.Simulation Results and Discussions

In this section, the simulated CERTS microgrid system was tested and evaluated during different operating conditions using the Matlab Simulink platform. The generated voltage, currents, and power are receded for different load conditions to evaluate the grid stability in isolates and grid-connected scenarios. A fault analysis study is carried out to highlight the challenges of traditional protection schemes.

In this section, the dynamic performance of the modeled CERT microgrid system is investigated under normal loading conditions, the transition from grid-connected to islanding mode, sudden change in loading values, different values of solar irradiation, and initialization of system from reset (zero initial conditions). The voltage and current signals at the four main buses of the microgrid (Bus1, Bus2, Bus 3, Bus4) are recorded for each case (refer to Fig. 1).

A. Normal loading condition

During grid-connected mode, the microgrid with its full load is initiated from rest with zero initial conditions, it can be noticed that the modeled system could reach its steady state values within 0.25sec, see Fig. 5 a & b. Also, the microgrid system reached its steady state values during islanding mode within 0.25 sec as indicated in Fig. 6 a & b. The current and voltage waveforms take about 0.25 seconds as a transient period to reach their steady-state values.

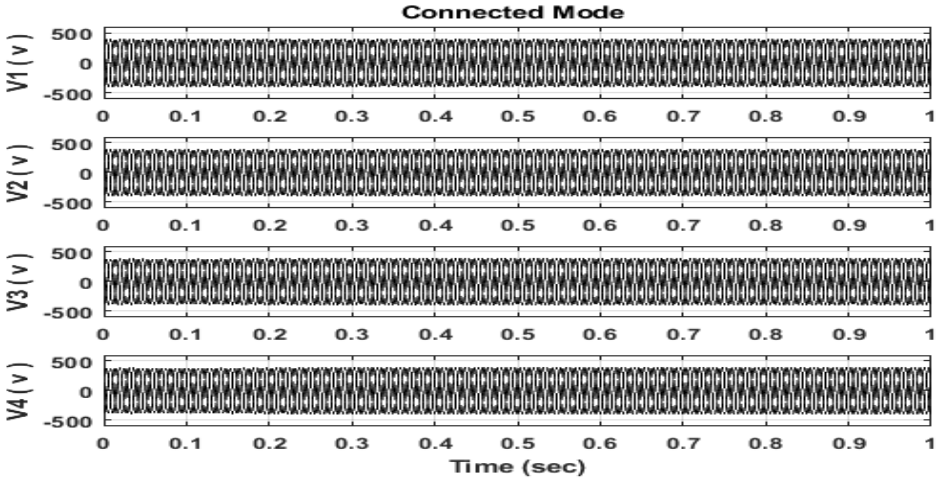

a) Voltage waveforms.

How to Cite this Article:

Awaad, I., Mansour, N. and Abdelsalam, A. (2024) 'Modeling and Performance Analysis of CERT Microgrid', Energy and Environmental Science Journal, 2(1), pp. 108–127. doi:10.21608/sceee.2024.294186.1029.

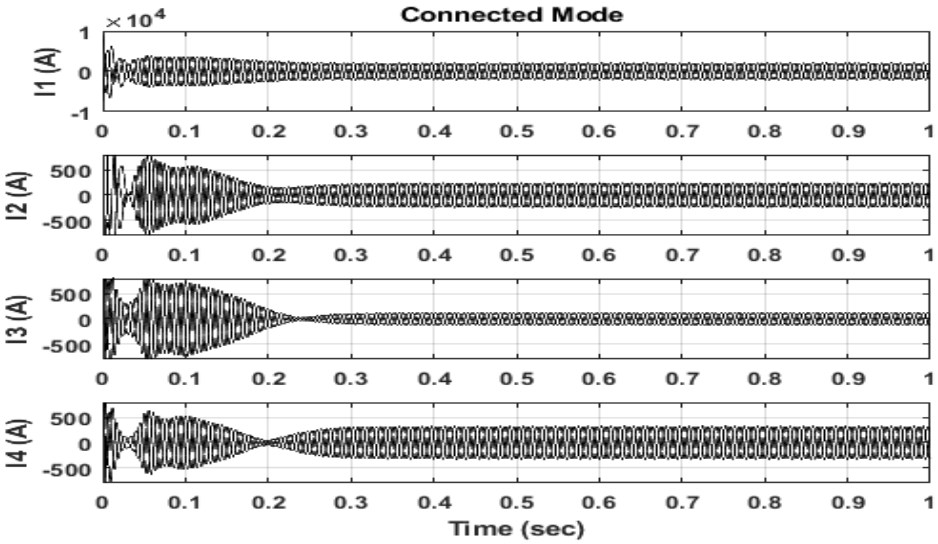

b) Current waveforms.

Figure. 5 Voltage and current waveforms of the micro-grid system measured at Bus1-Bus 4 during initialization of the grid-connected condition.

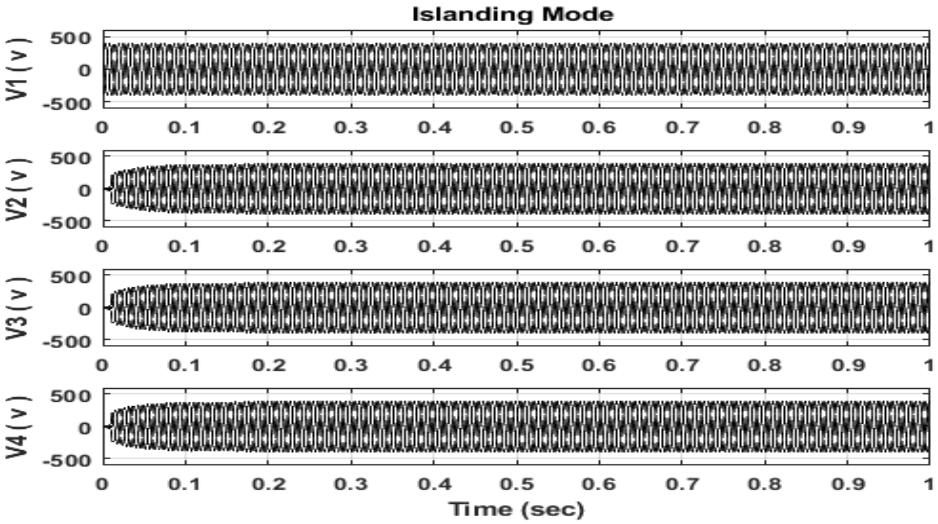

a) Voltage waveforms.

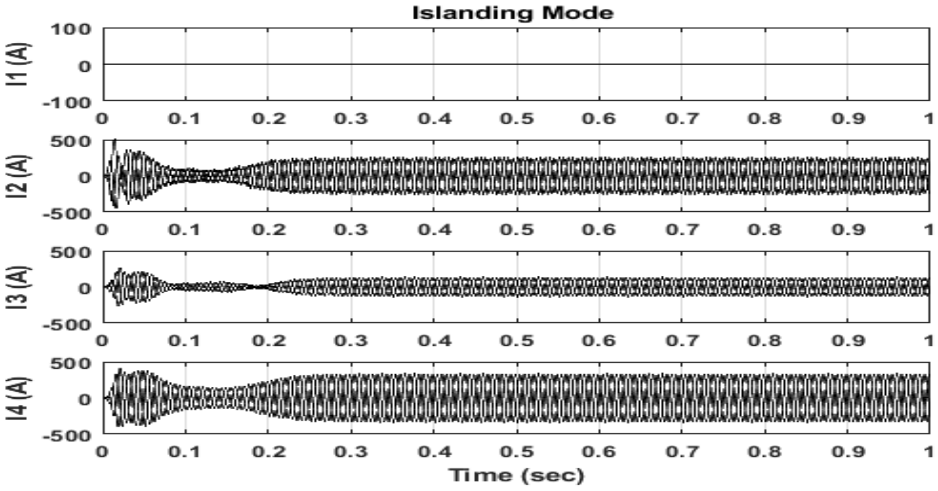

b) Current waveforms.

Figure. 6 Voltage and current waveforms of the micro-grid system measured at Bus1-Bus 4 during initialization of the islanding mode condition.

How to Cite this Article:

Awaad, I., Mansour, N. and Abdelsalam, A. (2024) 'Modeling and Performance Analysis of CERT Microgrid', Energy and Environmental Science Journal, 2(1), pp. 108–127. doi:10.21608/sceee.2024.294186.1029.

B. Transition from grid-connected to islanding mode

The stability of the modeled CERT microgrid system is tested during the transition from grid-connected mode to islanding mode. As shown in Fig. 7, if the microgrid is disconnected from the main grid after 0.7sec, it can restore its steady state within 0.8sec. The voltage waveforms are exposed to a slight change in their magnitudes at the instant of isolation, but they quickly regain their steady-state values within 0.8sec as shown in Fig. 7. a. Also, the current waveforms were rabidly increased at the moment of isolation, but they regained their steady values within 0.8 sec, as in Fig. 7. b.

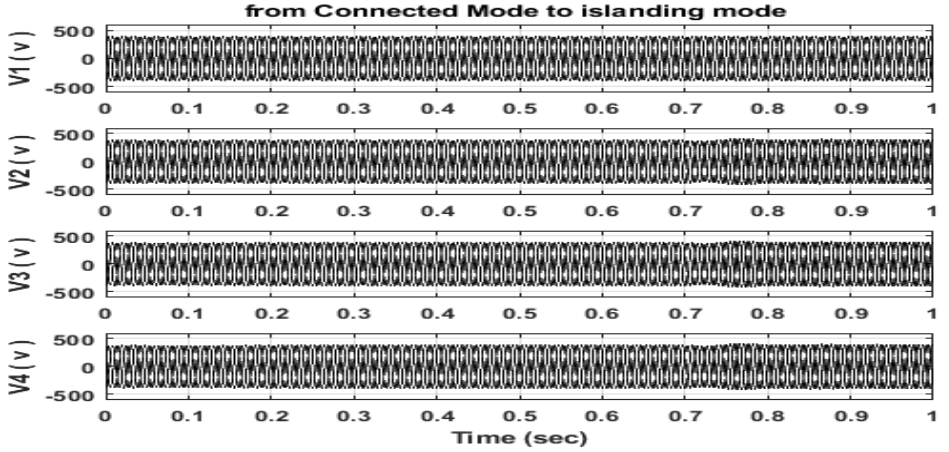

a) Voltage waveforms.

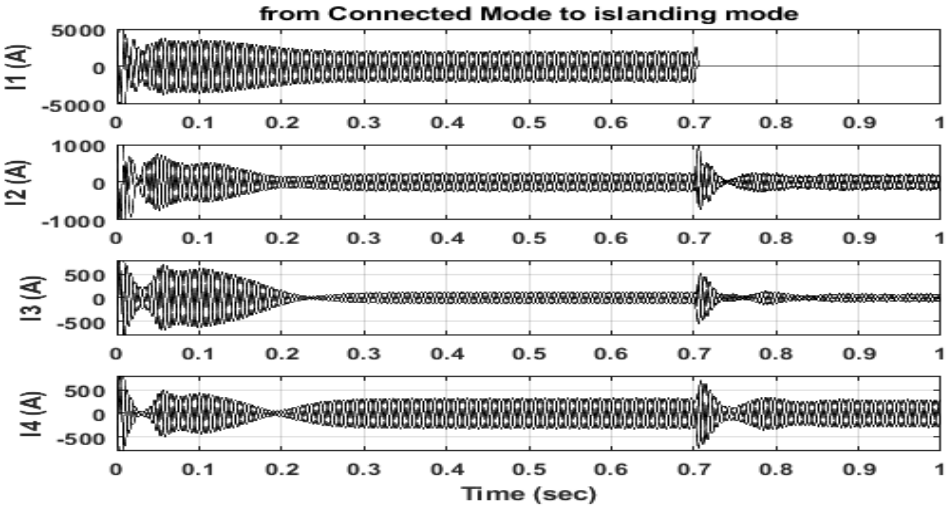

b) **Current waveforms**.

Figure. 7 Voltage and current waveforms of the micro-grid system measured at Bus1-Bus 4 during the transition from grid-connected mode to islanding mode.

c) Sudden change in loading values

In grid-connected mode, if the additional load is added in parallel with load 3 (L3) at 0.7 sec, the voltage waveforms could keep their stable values as in Fig. 8. a, and the electrical current drawn from the grid increased, and this appeared to increase in Bus 1 and Bus 2 currents as in Fig. 8. b. In contrast, the voltage magnitude shows a reasonable decrease at the moment of load change during islanding mode as in Fig. 9. a, and the current magnitude of the current measured at all the microgrid buses is increased as in Fig. 9. b. The CERT microgrid system could maintain its stability during load change.

How to Cite this Article:

Awaad, I., Mansour, N. and Abdelsalam, A. (2024) 'Modeling and Performance Analysis of CERT Microgrid', Energy and Environmental Science Journal, 2(1), pp. 108–127. doi:10.21608/sceee.2024.294186.1029.

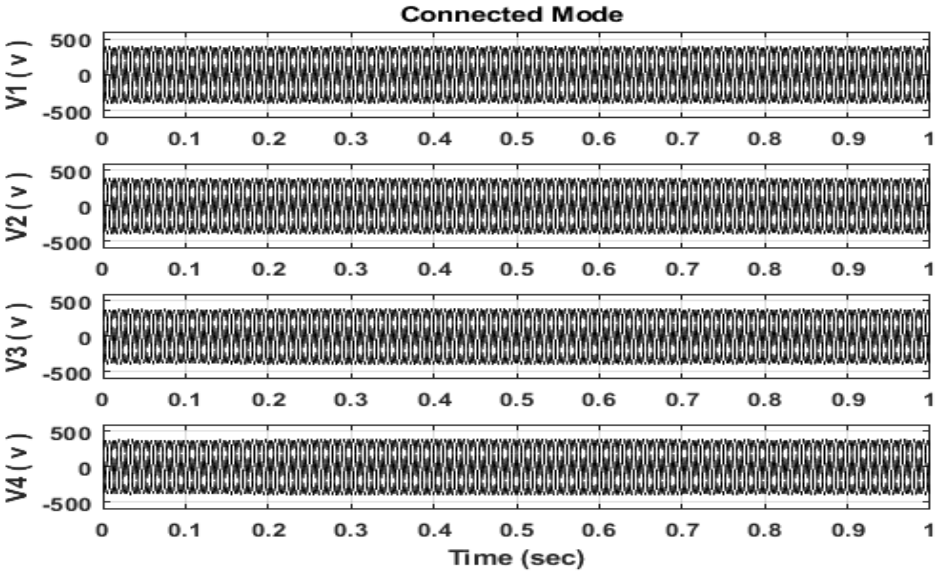

a) Voltage waveform.

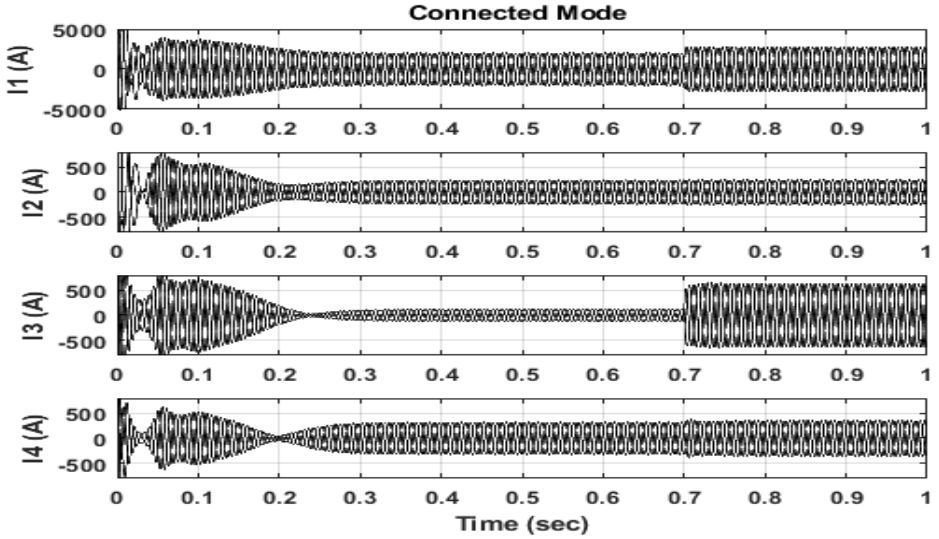

b) Current waveforms.

Figure. 8 Voltage and current waveforms of the micro-grid system measured at Bus1-Bus 4 for the sudden change in load magnitude during the grid-connected mode.

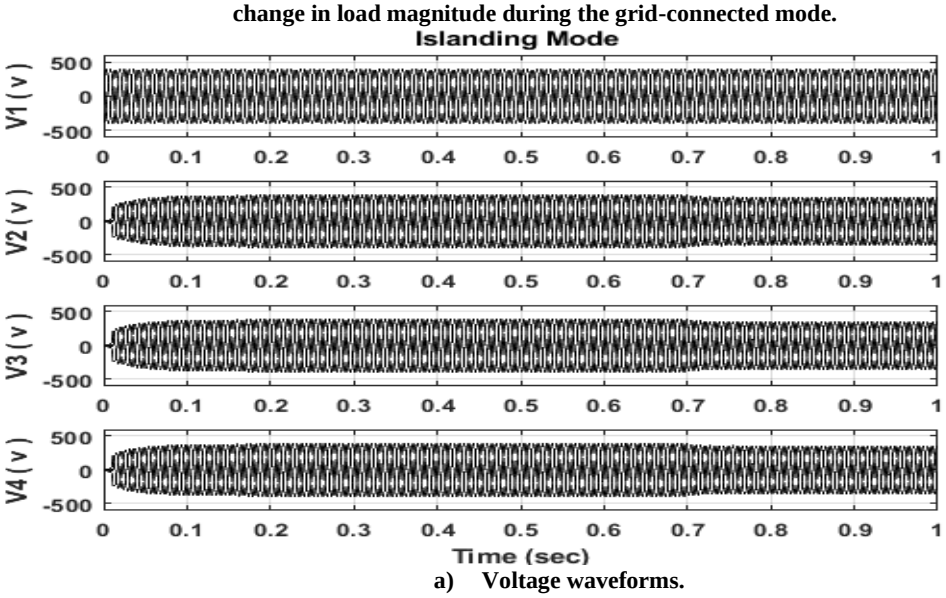

a) Voltage waveforms.

How to Cite this Article:

Awaad, I., Mansour, N. and Abdelsalam, A. (2024) 'Modeling and Performance Analysis of CERT Microgrid', Energy and Environmental Science Journal, 2(1), pp. 108–127. doi:10.21608/sceee.2024.294186.1029.

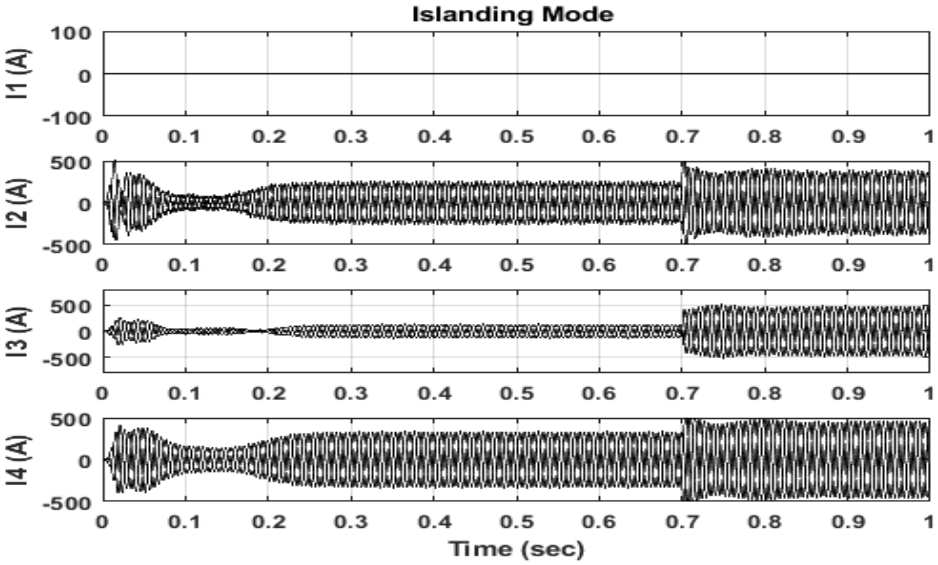

b) Current waveforms.

Figure. 9 Voltage and current waveforms of the micro-grid system measured at Bus1-Bus 4 during a sudden change in load magnitude in islanding mode.

c) Change of solar irradiance

The solar irradiance variation effects on the response of the CERT microgrid system during grid-connected and islanding modes are indicated in Fig. 10 & 11. The irradiation value is increased from 600 w/m2 to 800 w/m^2 at 0.5 sec, the CERT microgrid system is responding to this increase by the current magnitude increasing.

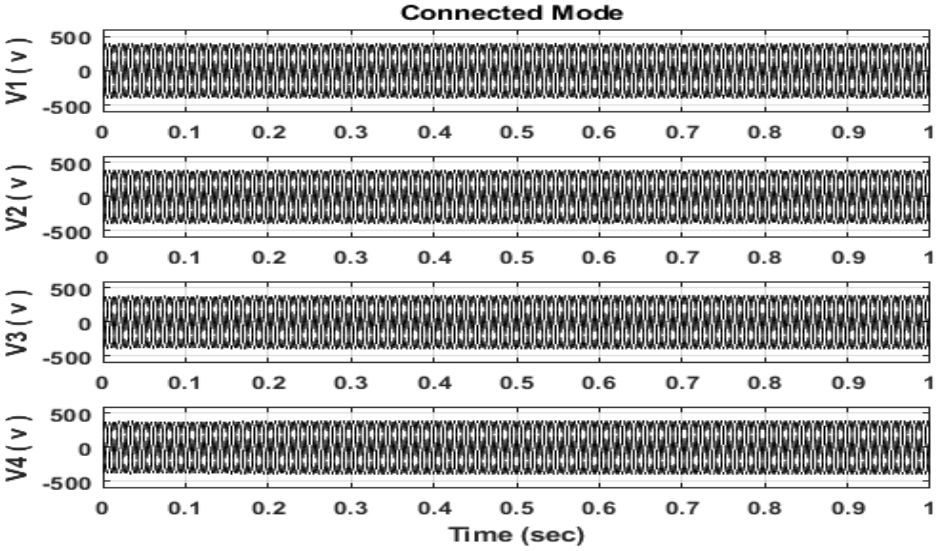

a) Voltage waveforms.

How to Cite this Article:

Awaad, I., Mansour, N. and Abdelsalam, A. (2024) 'Modeling and Performance Analysis of CERT Microgrid', Energy and Environmental Science Journal, 2(1), pp. 108–127. doi:10.21608/sceee.2024.294186.1029.

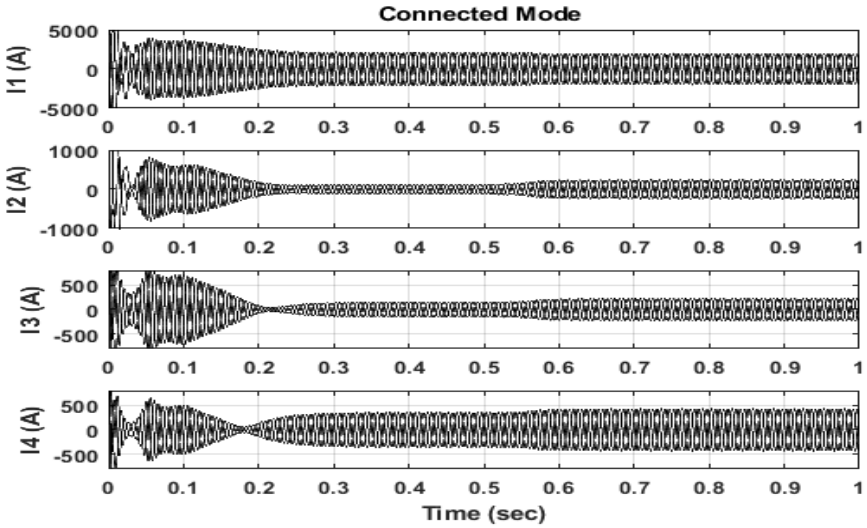

b) Current waveforms.

Figure. 10 Voltage and current waveforms of the micro-grid system measured at Bus1-Bus 4 for the sudden change in solar irradiance magnitude at 0.5sec during grid-connected mode.

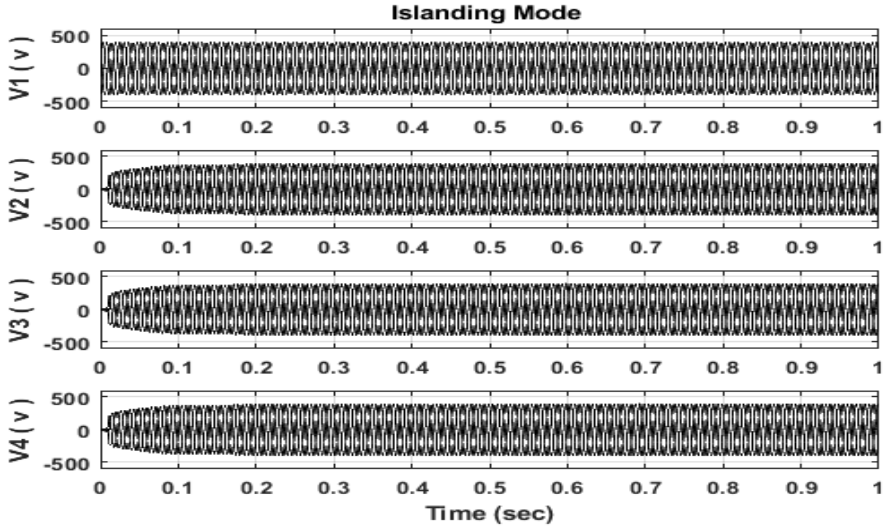

a) Voltage waveforms.

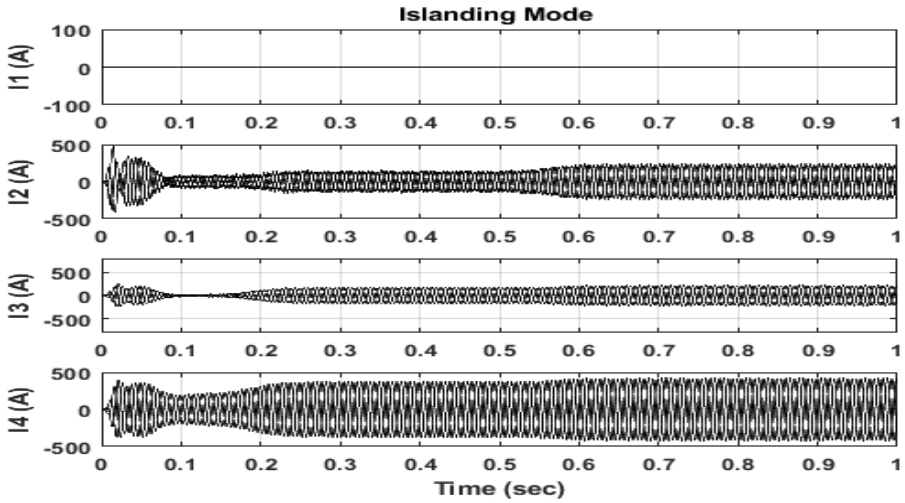

b) Current waveforms.

Fig. 11 Voltage and current waveforms of the micro-grid system measured at Bus1-Bus 4 for the sudden change in solar irradiance magnitude at 0.5sec during the islanding mode.

How to Cite this Article:

Awaad, I., Mansour, N. and Abdelsalam, A. (2024) 'Modeling and Performance Analysis of CERT Microgrid', Energy and Environmental Science Journal, 2(1), pp. 108–127. doi:10.21608/sceee.2024.294186.1029.

c) Fault analysis study

The three-phase short circuit at the mid-point of the feeder T22 during the grid-connected and islanding modes is carried out, and the voltage and current magnitudes are recorded as in Figs. 12 and 13. It can be noticed that the steady-state fault current level recorded at Bus 2 for grid-connected mode is greater than that for islanding mode due to the fault current support from the grid. In the grid-connected mode, the fault current level could be easily detected by the traditional overcurrent protection scheme, and the fault could be successfully isolated.

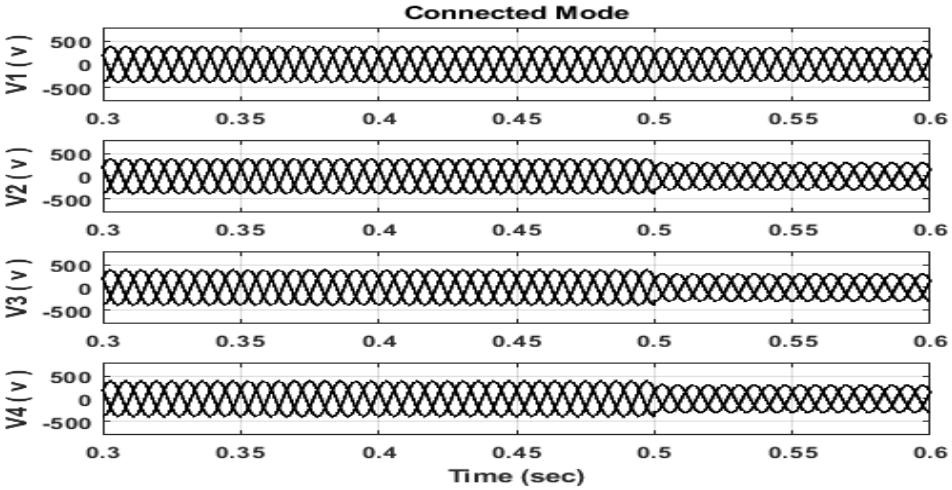

a) Voltage waveforms.

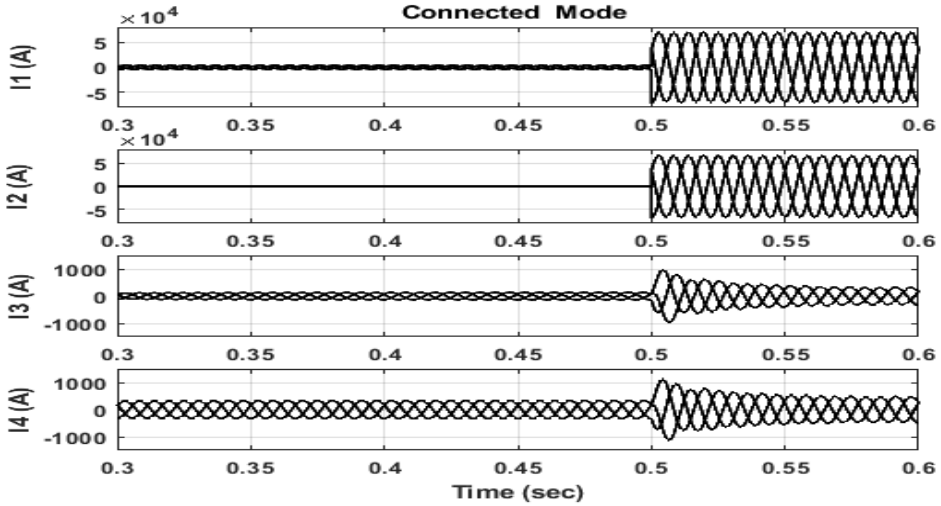

b) Current waveforms.

Figure. 12 Voltage and current waveforms of the micro-grid system measured at Bus1-Bus 4 for solidly ABC fault at the mid-point of feeder T22 during grid-connected mode.

How to Cite this Article:

Awaad, I., Mansour, N. and Abdelsalam, A. (2024) 'Modeling and Performance Analysis of CERT Microgrid', Energy and Environmental Science Journal, 2(1), pp. 108–127. doi:10.21608/sceee.2024.294186.1029.

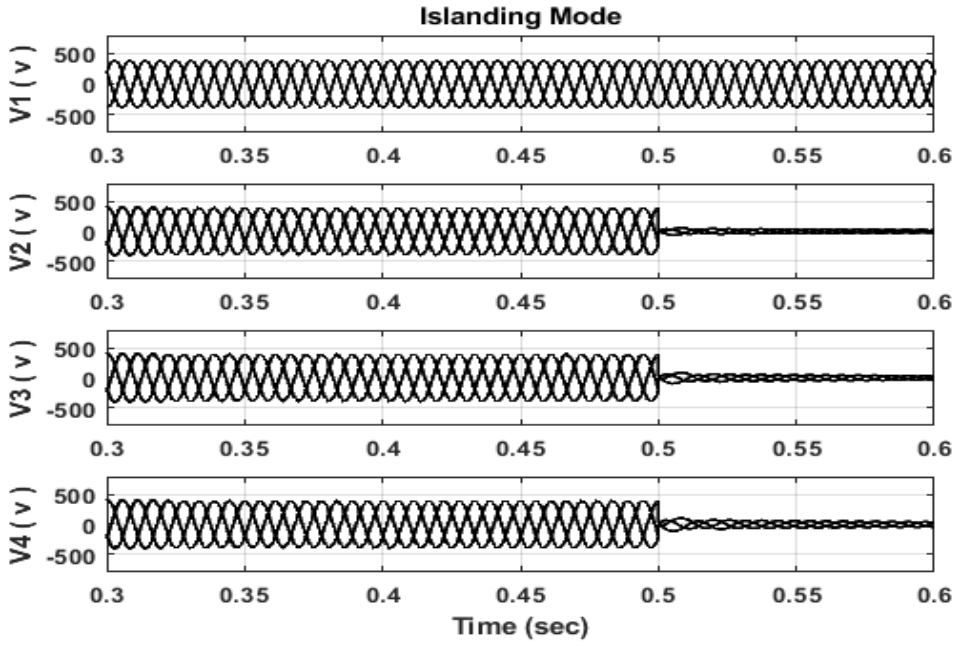

a) Voltage waveforms.

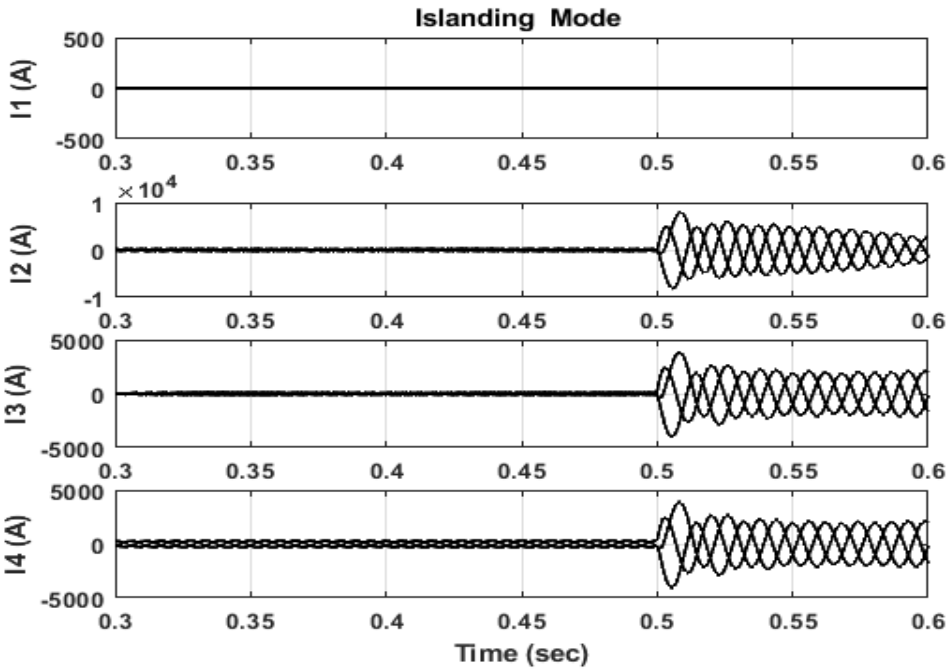

b) Current waveforms.

Figure. 13 Voltage and current waveforms of the micro-grid system measured at Bus1-Bus 4 for solidly ABC fault at the mid-point of feeder T22 during islanding mode.

In contrast, the steady-state fault current level during island mode that is recorded at Bus 2 (I_2) is decreased, and its magnitude may not be detected by the traditional overcurrent relay scheme. However, the three-phase fault in both grid-connected and islanding modes could be successfully detected; the situation will be worse if the fault resistance is considered, especially in islanding mode. Fig. 12 shows that despite a three-phase fault at Bus 2, which is close to the point of common coupling (PCC), the grid support prevents a significant reduction in voltage. On the other hand, because of its distance from the grid, the voltage decreases for the identical fault at line T44's midpoint is noteworthy; see Fig. 14, the voltage magnitude at Bus 4 (V4). The fault current magnitudes recorded for the islanding mode are large and the fault could be isolated with the traditional protection schemes, see Fig. 15.

How to Cite this Article:
Awaad, I., Mansour, N. and Abdelsalam, A. (2024) 'Modeling and Performance Analysis of CERT Microgrid', Energy and Environmental Science Journal, 2(1), pp. 108–127. doi:10.21608/sceee.2024.294186.1029.

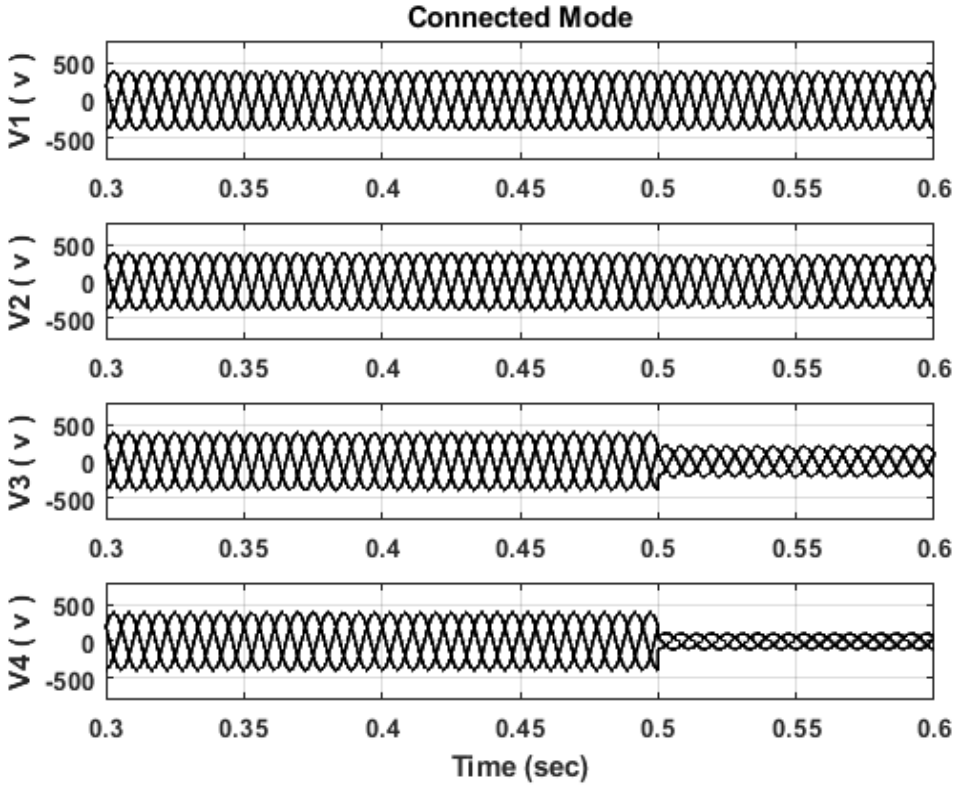

a) Voltage waveforms.

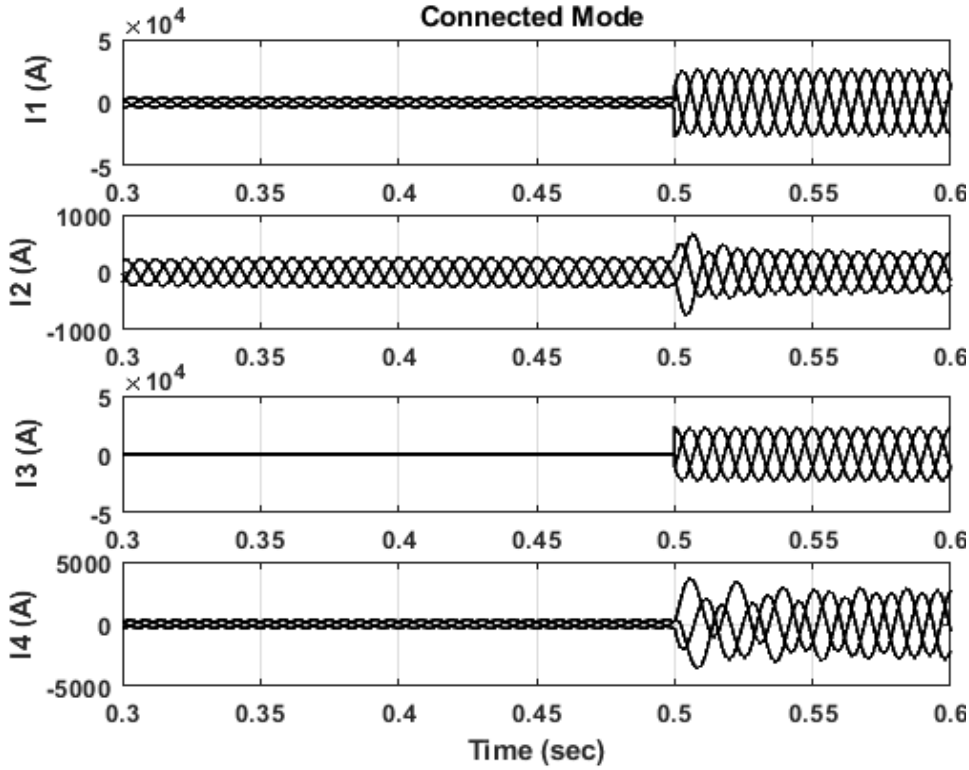

b)Current waveforms.

Figure. 14 Voltage and current waveforms of the micro-grid system measured at Bus1-Bus 4 for solidly ABC fault at the mid-point of feeder T44 during grid-connected mode.

How to Cite this Article:

Awaad, I., Mansour, N. and Abdelsalam, A. (2024) 'Modeling and Performance Analysis of CERT Microgrid', Energy and Environmental Science Journal, 2(1), pp. 108–127. doi:10.21608/sceee.2024.294186.1029.

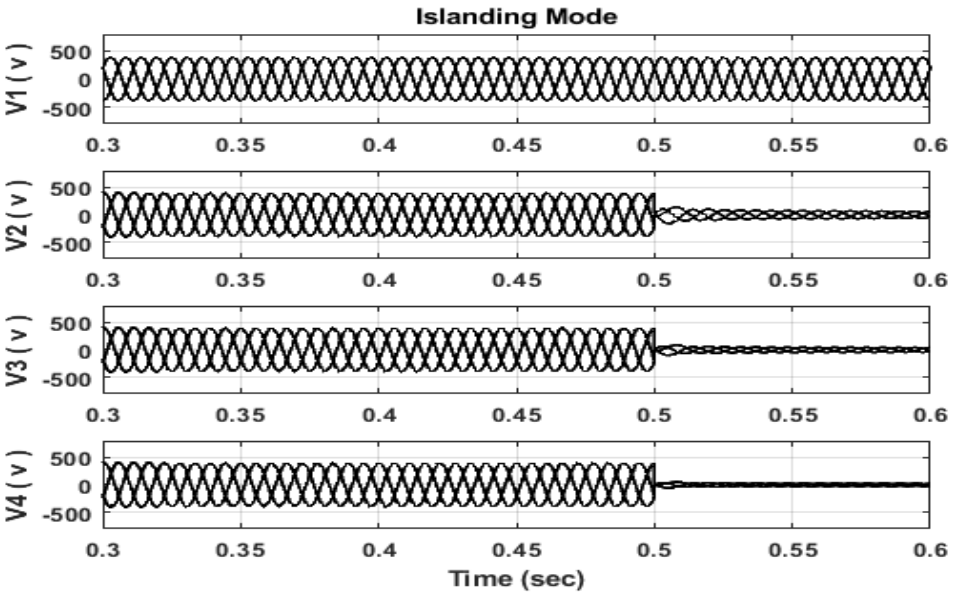

a) Voltage waveforms.

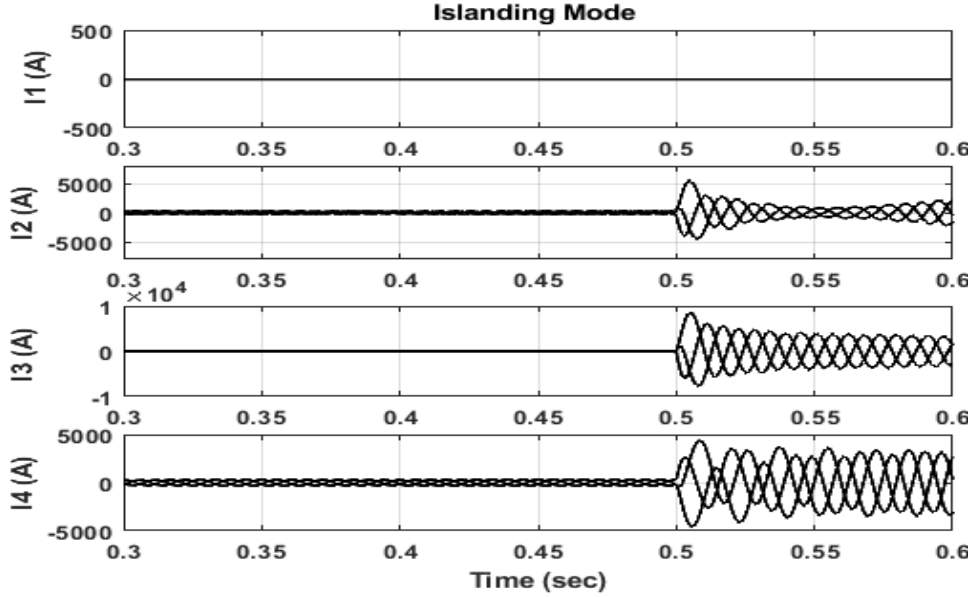

b) Current waveforms.

Figure. 15 Voltage and current waveforms of the micro-grid system measured at Bus1-Bus 4 for solidly ABC fault at the mid-point of feeder T44 during islanding mode.

Traditionally, the short feeders are usually protected by a simple overcurrent protection scheme that is initiated by the fault current magnitude. If the fault resistance is considered, the traditional protection scheme will not be sufficient for a microgrid system in islanding mode.

The same responses for solidly AB fault at the midpoint of feeder T44 are achieved, the fault current level is decreased in the islanding mode w.r.t grid-connected mode as in Figs. 16 and 17.

How to Cite this Article:

Awaad, I., Mansour, N. and Abdelsalam, A. (2024) 'Modeling and Performance Analysis of CERT Microgrid', Energy and Environmental Science Journal, 2(1), pp. 108–127. doi:10.21608/sceee.2024.294186.1029.

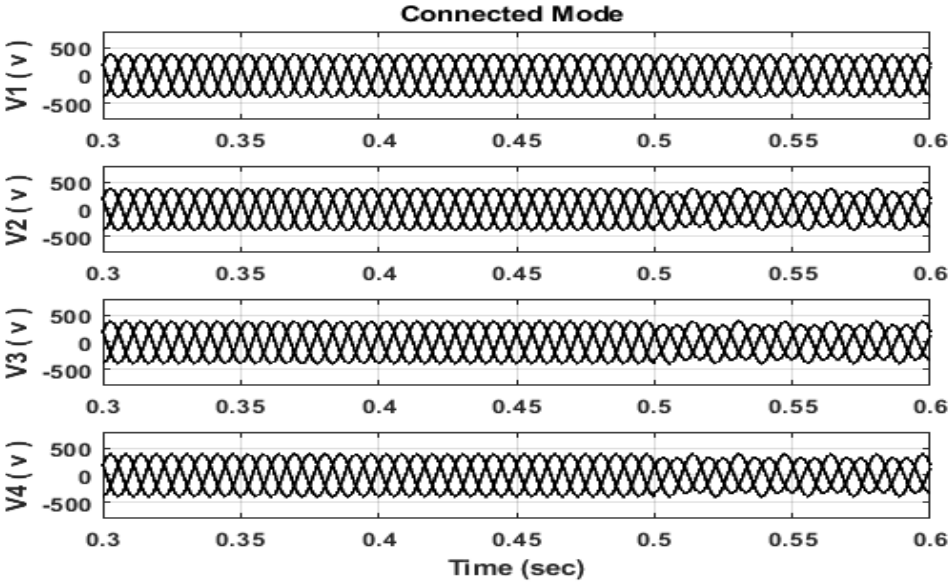

a) Voltage waveforms.

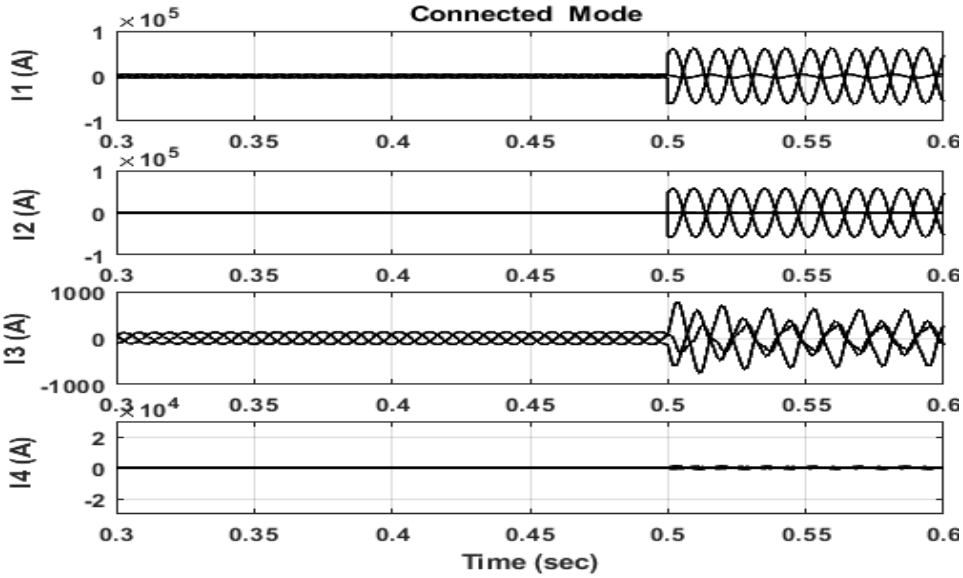

b) Current waveforms.

Figure. 16 Voltage and current waveforms of the micro-grid system measured at Bus1-Bus 4 for solidly AB fault at the mid-point of feeder T22 during grid-connected mode.

How to Cite this Article:

Awaad, I., Mansour, N. and Abdelsalam, A. (2024) 'Modeling and Performance Analysis of CERT Microgrid', Energy and Environmental Science Journal, 2(1), pp. 108–127. doi:10.21608/sceee.2024.294186.1029.

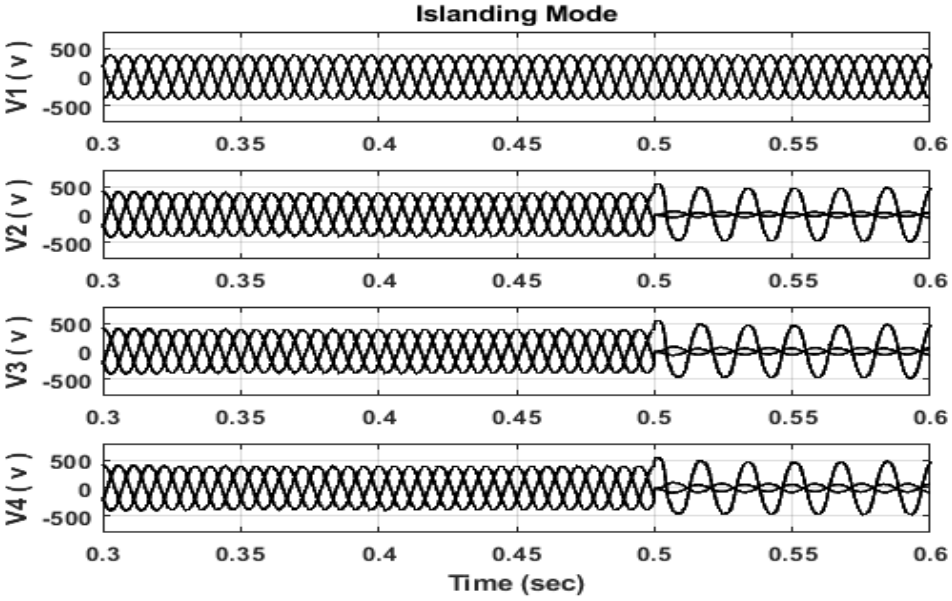

a) Voltage waveforms.

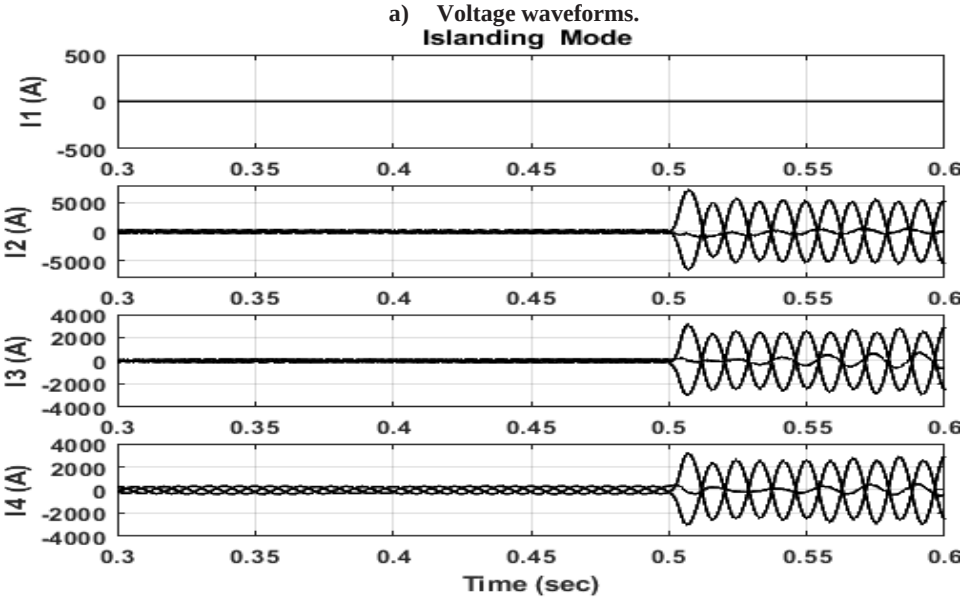

b) Current waveforms.

Figure. 17 Voltage and current waveforms of the micro-grid system measured at Bus1-Bus 4 for solidly AB fault at the mid-point of feeder T22 during islanding mode.

How to Cite this Article:

Awaad, I., Mansour, N. and Abdelsalam, A. (2024) 'Modeling and Performance Analysis of CERT Microgrid', Energy and Environmental Science Journal, 2(1), pp. 108–127. doi:10.21608/sceee.2024.294186.1029.

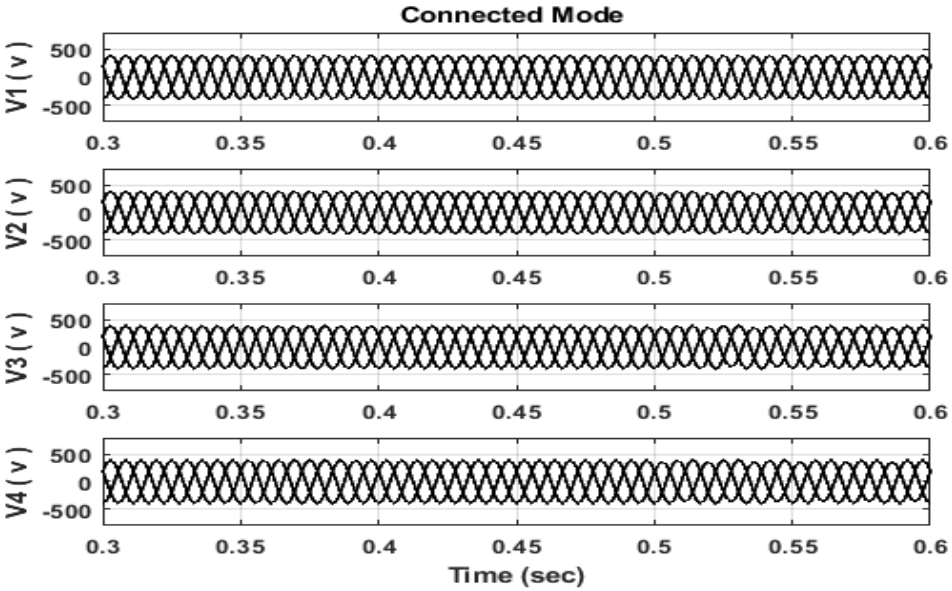

a) Voltage waveforms.

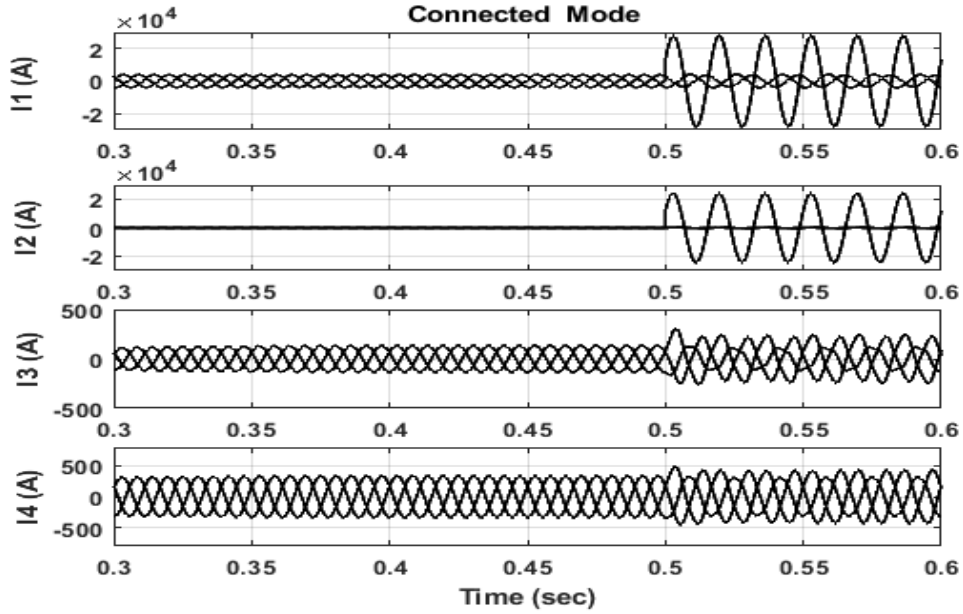

b) **Current waveforms.**

Figure. 18 Voltage and current waveforms of the micro-grid system measured at Bus1-Bus 4 for solidly AG fault at the mid-point of feeder T22 during grid-connected mode.

The situation is worsened for phase-to-ground faults; an AG fault occurs at the midpoint of feeder T22; the voltage magnitude in the case of grid-connected is slightly affected; and the fault current contribution from the grid is high and can be detected as shown in Fig. 18. In contrast, the fault current contribution from the DERs during islanding mode is insufficient to be detected by the traditional protection elements, as shown in Fig. 19. Also, there is a sensible overvoltage in the healthy phases in the islanding mode.

How to Cite this Article:

Awaad, I., Mansour, N. and Abdelsalam, A. (2024) 'Modeling and Performance Analysis of CERT Microgrid', Energy and Environmental Science Journal, 2(1), pp. 108–127. doi:10.21608/sceee.2024.294186.1029.

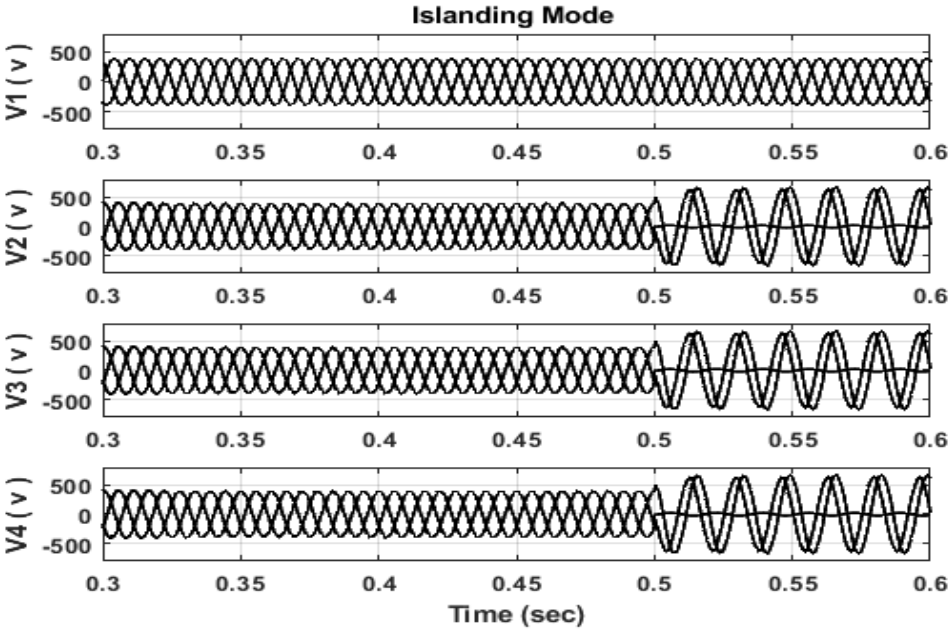

a) Voltage waveforms.

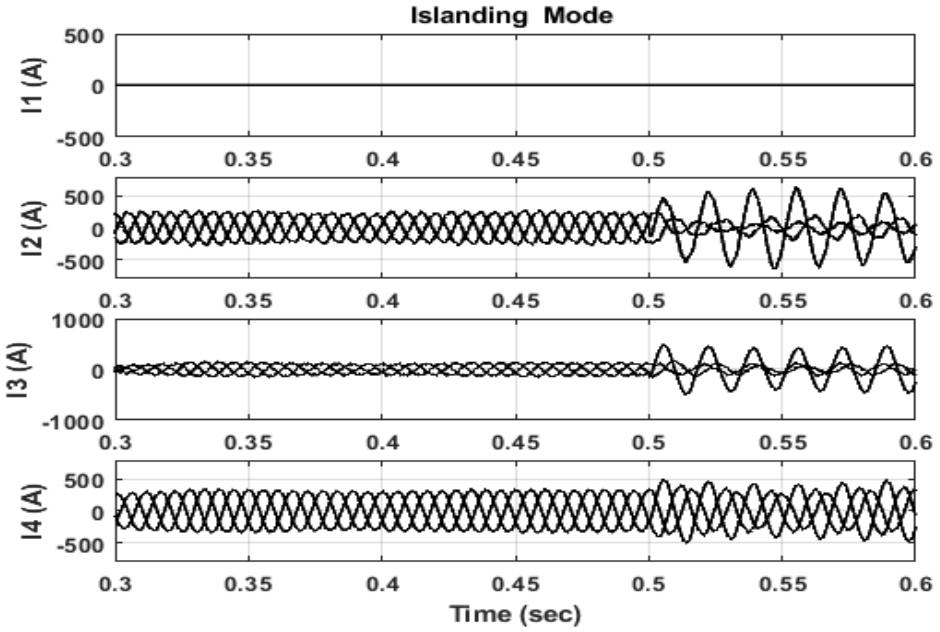

b) Current waveforms.

Figure. 19 Voltage and current waveforms of the micro-grid system measured at Bus1-Bus 4 for solidly AG fault at the mid-point of feeder T22 during islanding mode.

IV. CONCLUSION

In this paper, an effective model of the CERTS microgrid testbed system is introduced. The model is tested in both grid-connected and islanding modes for different normal and up-normal conditions. The stability of the model and the evaluation of the DER-controller during varying load values, variation of solar irradiance, and transition from grid-connected to islanding mode. The introduced model is used to evaluate the performance of the overcurrent scheme traditionally used in short feeder protection. A detailed fault analysis study is carried out through the modeling of different fault types at different locations during the grid-connected and islanding modes. The study concluded that the traditional protection scheme based on overcurrent relays was unable to provide efficient protection for microgrids during the islanding mode. So, the smart protection scheme is required for perfect fault detection, classification, and isolation of microgrids during islanding mode.

How to Cite this Article:

Awaad, I., Mansour, N. and Abdelsalam, A. (2024) 'Modeling and Performance Analysis of CERT Microgrid', Energy and Environmental Science Journal, 2(1), pp. 108–127. doi:10.21608/sceee.2024.294186.1029.

REFERENCES

[1]. Barra, P., Coury, D., & Fernandes, R. (2020). A survey on adaptive protection of microgrids and distribution systems with distributed generators. Renewable and Sustainable Energy Reviews, 118, 109524. https://doi.org/ 10.1016/j.rser.2019.109524

[2]. D.E. Olivares, A. Mehrizi-Sani, A.H. Etemadi, C.A. Canizares, R. Iravani, M. Kazerani, A.H. Hajimiragha, O. Gomis-Bellmunt, M. Saeedifard, R. Palma-Behnke, G.A. Jimenez-Estevez, N.D. Hatziargyriou, "Trends in Microgrid Control," IEEE Trans. Smart Grid, vol. 5, no. 4, pp. 1905-1919, July 2014

[3]. R. H. Lasseter, "MicroGrids," in Proc. IEEE Power Eng. Soc. Winter Meeting, Jan. 2002, vol. 1, pp. 305–308.

[4]. Gopalan, S., Sreeram, V., & Iu, H. (2014). A review of coordination strategies and protection schemes for microgrids. Renewable and Sustainable Energy Reviews, 32, 222–228. https://doi.org/10.1016/j.rser.2014.01.037,

[5]. Sedhom, B., El-Saadawi, M., El Moursi, M., Hassan, M., & Eladl, A. (2021). IoT-based optimal demand side management and control scheme for smart microgrid. International Journal of Electrical Power & Energy Systems, 127, 106674. https://doi.org/10.1016/j.ijepes.2020.106674

[6]. G. Shahgholian, A brief review on microgrids: Operation, applications, modeling, and control, Int. Trans. Electr. Energy Syst. (2021) e12885.

[7]. J. Hu, T. Zhang, S. Du, Y. Zhao, An overview on analysis and control of the micro-grid system, Int. J. Control Autom. 8 (6) (2015) 65–76.

[8]. Singh, I. Elamvazuthi, P. Nallagownden, G. Ramasamy, A. Jangra, Routing-based multi-agent system for network reliability in the smart microgrid, Sensors 20 (10) (2020) 2992.

[9]. Y. Yoldaş, A. Önen, S. M. Muyeen, A. v. Vasilakos, and İ. Alan, 'Enhancing smart grid with microgrids: Challenges and opportunities, Renewable and Sustainable Energy Reviews, vol. 72. Elsevier Ltd, pp. 205–214, 2017. Doi: 10.1016/j.rser.2017.01.064.

[10]. X. Kang, C. E. K. Nuworklo, B. S. Tekpeti, and M. Kheshti, 'Protection of micro-grid systems: a comprehensive survey, The Journal of Engineering, vol. 2017, no. 13, pp. 1515–1518, Jan. 2017, Doi: 10.1049/joe.2017.0584.

[11]. IEEE Staff and IEEE Staff, 2012 IEEE Power and Energy Society General Meeting.

[12]. P. Basak, S. Chowdhury, S. Halder Nee Dey, and S. P. Chowdhury, 'A literature review on integration of distributed energy resources in the perspective of control, protection, and stability of microgrid', Renewable and Sustainable Energy Reviews, vol. 16, no. 8. pp. 5545–5556, Oct. 2012. Doi: 10.1016/j.rser.2012.05.043.

[13]. R. Lasseter, A. Akhil, C. Marnay, J. Stephens, J. Dagle, R. Guttromsom, A. S. Meliopoulous, R. Yinger, and J. Eto, "Integration of distributed energy resources - The CERTS microgrid concept," Lawrence Berkeley National Lab. (LBNL), Berkeley, CA (United States), Tech. Rep., 2002.

[14]. D. K. Nichols, J. Stevens, R. H. Lasseter, J. H. Eto, and H. T. Vollkommer, "Validation of the CERTS microgrid concept the CEC/CERTS microgrid testbed," 2006 IEEE Power Engineering Society General Meeting, Montreal, QC, Canada, 2006, pp. 3 pp.-, doi: 10.1109/PES.2006.1709248.

[15]. J. Eto et al., "Overview of the CERTS Microgrid Laboratory Test Bed," 2009 CIGRE/IEEE PES Joint Symposium Integration of Wide-Scale Renewable Resources Into the Power Delivery System, Calgary, AB, Canada, 2009, pp. 1-1.

[16]. Ranjit, Ajit A., Mahesh S. Illindala, and Abrez Mondal. "CERTS microgrid: Modeling analysis and control of distributed energy resources—Phase I." Lawrence Berkeley National Laboratory, Berkeley, CA, USA (2015).

[17]. Ranjit, Ajit A., Mahesh S. Illindala, and David A. Klapp. "Modeling and analysis of the CERTS microgrid with natural gas-powered distributed energy resources." 2015 IEEE/IAS 51st Industrial & Commercial Power Systems Technical Conference (I&CPS). IEEE, 2015.

[18]. Alegria, Eduardo, Anthony Ma, and Osama Idrees. CERTS Microgrid Demonstration with Large-scale Energy Storage and Renewables at Santa Rita Jail: Final Project Report. Vol. 1. State of California Energy Commission, 2014.

[19]. Johnson, Brian, et al. "A unified dynamic characterization framework for microgrid systems." Electric Power Components and Systems 40.1 (2011): 93-111.

[20]. Umar, Muhammad. Modeling and simulation of The CERTS Microgrid: a comparative study using PSCAD and MATLAB SIMSCAPE. University of Ontario Institute of Technology (Canada), Doctoral dissertation) 2020.

[21]. Abdelgayed, Tamer S., Walid G. Morsi, and Tarlochan S. Sidhu. "A new approach for fault classification in microgrids using optimal wavelet functions matching pursuit." IEEE Transactions on Smart Grid 9.5 (2017): 4838-4846.

[22]. R. H. Lasseter, J. H. Eto, B. Schenkman, J. Stevens, H. Vollkommer, D. Klapp, et al., "CERTS microgrid laboratory test bed," IEEE Trans. Power Del., vol. 26, no. 1, pp. 325–332, Jan. 2011.

[23]. Rayane Mourouvin, Juan Carlos Gonzalez-Torres, Jing Dai, Abdelkrim Benchaib, Didier Georges, et al. Understanding the role of VSC control strategies in the limits of power electronics integration in AC grids using modal analysis. Electric Power Systems Research, 2021, 192 (March), pp.106930. 10.1016/j.epsr.2020.106930. hal-03651565.

How to Cite this Article:

Awaad, I., Mansour, N. and Abdelsalam, A. (2024) 'Modeling and Performance Analysis of CERT Microgrid', Energy and Environmental Science Journal, 2(1), pp. 108–127. doi:10.21608/sceee.2024.294186.1029.

[24]. I. Colak, “Introduction to smart grid,” in 2016 International Smart Grid Workshop and Certificate Program (ISGWCP), Istanbul, Turkey, 2016, pp. 1–5, doi: 10.1109/ISGWCP.2016.7548265.

[25]. Yazdani, and R. Iravani, Voltage-sourced converters in power systems: modeling, control, and applications. John Wiley & Sons, Mar. 2010.

[26]. Saad, E., Elkoteshy, Y., & AbouZayed, U. (2020). Modeling and analysis of grid-connected solar-PV system through current-mode controlled VSC. In E3S Web of Conferences (Vol. 167, p. 05005). EDP Sciences.

[27]. A. Yazdani and P. Dash, “A control methodology and characterization of dynamics for a photovoltaic (PV) system interfaced with a distribution network,” IEEE Trans. Power Del., vol. 24, no. 3, pp. 1538– 1555, Jul. 2009.

How to Cite this Article:

Awaad, I., Mansour, N. and Abdelsalam, A. (2024) ‘Modeling and Performance Analysis of CERT Microgrid’, Energy and Environmental Science Journal, 2(1), pp. 108–127. doi:10.21608/sceee.2024.294186.1029.